Nečas Center for Mathematical Modeling

C^2 Hermite interpolation by Pythagorean-hodograph quintic triarcs

B. Bastl, M. Bizzarri, B. Kovač, M. Krajnc, M. Lávička, K. Michálková, K. Počkaj, Z. Šír, E. Žagar

Preprint no. 2014-09

http://ncmm.karlin.mff.cuni.cz/

C^2 Hermite interpolation by Pythagorean-hodograph quintic triarcs

Bohumír Bastl[a,b], Michal Bizzarri[b,a], Boštjan Kovač[e], Marjeta Krajnc[c], Miroslav Lávička[a,b], Kristýna Michálková[b,a,*], Karla Počkaj[d], Zbyněk Šír[a], Emil Žagar[c]

[a]*University of West Bohemia, Faculty of Applied Sciences, Department of Mathematics, Univerzitní 8, Plzeň, Czech Republic*
[b]*University of West Bohemia, NTIS, Faculty of Applied Sciences, Univerzitní 8, Plzeň, Czech Republic*
[c]*University of Ljubljana, IMFM and FMF, Jadranska 19, Ljubljana, Slovenia*
[d]*University of Primorska, IAM, Muzejski trg 2, Koper, Slovenia*
[e]*Abelium d.o.o., Kajuhova 90, Ljubljana, Slovenia*

Abstract

In this paper, the problem of C^2 Hermite interpolation by triarcs composed of Pythagorean-hodograph (PH) quintics is considered. The main idea is to join three arcs of PH quintics at two unknown points – the first curve interpolates given C^2 Hermite data at one side, the third one interpolates the same type of given data at the other side and the middle arc is joined together with C^2 continuity to the first and the third arc. For any set of C^2 planar boundary data (two points with associated first and second derivatives) we construct four possible interpolants. The best possible approximation order is 4. Analogously, for a set of C^2 spatial boundary data we find a six-dimensional family of interpolating quintic PH triarcs. The results are confirmed by several examples.

Keywords:
Pythagorean-hodograph curves, Hermite interpolation, triarc, PH quintic

1. Introduction

Shapes (curves, surfaces, volumes) in Computer Aided Geometric Design (CAGD), and in a vast variety of subsequent applications, are often described by piecewise polynomial/rational representations. However, not every shape can be represented using polynomial/rational functions, see [1] for more details. Another problem in CAGD is that many natural geometric operations, such as offsetting, do not preserve rationality of derived objects. Nonetheless, offsets to certain special classes of shapes admit exact rational representations.

In the case of planar curves, the class of Pythagorean-hodograph (PH) curves as polynomial curves possessing rational offset curves and polynomial arc-length functions was introduced in [2]. A thorough analysis of PH curves followed; see, e.g., [3–5]. The concept of planar PH curves was later generalized to polynomial spatial PH curves in [6, 7]. These curves have the following attractive properties: the arc length of any segment can be determined exactly without numerical approximation and any canal surface based on spatial PH curves as its spine has a precise rational parameterization. The case of PH curves in $\mathbb{R}^n$ for $n > 3$ is still not solved satisfactorily. Exploiting recent results from number theory, the structure of PH curves in dimensions $n = 5$ and $n = 9$ was characterized in [8, 9]. We would like to recall that polynomial PH curves have their counterparts also in rational versions – see [10–13] for more details on rational planar PH curves, and [14] where rational spatial PH curves were introduced and studied. However rational PH curves are beyond the scope of this paper. A detailed survey of the literature on shapes with a Pythagorean property and their applications in technical practice can be found in [15].

*Corresponding author
Email addresses: bastl@kma.zcu.cz (Bohumír Bastl), bizzarri@kma.zcu.cz (Michal Bizzarri), bostjan.kovac@abelium.eu (Boštjan Kovač), marjetka.krajnc@fmf.uni-lj.si (Marjeta Krajnc), lavicka@kma.zcu.cz (Miroslav Lávička), kslaba@kma.zcu.cz (Kristýna Michálková), karla.pockaj@upr.si (Karla Počkaj), zsir@kma.zcu.cz (Zbyněk Šír), emil.zagar@fmf.uni-lj.si (Emil Žagar)

Many PH interpolation techniques (yielding C^1/G^1 or C^2/G^2 continuity) which form the cornerstone of subsequent approximation algorithms devoted to particular problems originating in technical practice have been formulated in recent years. These methods by planar or spatial polynomial PH curves are usually based on low degree polynomials – mainly 3 and 5 (in some cases also 7 and 9), as only odd degree PH curves are regular. For planar cubic PH curves one of the first interpolation methods was given in [16] where G^1 interpolation of Hermite data was analyzed. These results were generalized in [17] to G^2 interpolation by the same objects. Later the problem was revisited in [18, 19]. For quintic planar PH curves, several results on first and second order continuous spline interpolation are given in [5, 15, 20–23]. For spatial curves, G^1 Hermite interpolation by PH cubics was thoroughly investigated in [24]. Those results were later generalized to some level in [25]. The most general results on this type of interpolation can be found in [26] and [27]. The problem of C^1 and C^2 Hermite interpolation by spatial PH curves of degree ≥ 5 has been studied in [28–31].

C^1 Hermite interpolation by cubic polynomial spline curves is always uniquely solvable, so it is obvious that the same problem cannot be solved by PH cubic splines. However, cubic (i.e., low degree) polynomial interpolating splines are preferred in many applications. An interesting approach was used in [32], where C^1 Hermite interpolation via double-Tschirnhausen cubics (TC-biarcs) have been considered. The main idea was to join two arcs of planar cubic PH curves at some unknown point – the first curve interpolates C^1 Hermite data at one side, the other one interpolates the same type of data at the other side and the arcs are joined together with C^1 continuity. This approach was recently improved in [33], where planar uniform and non-uniform cubic PH biarcs were studied and applied. Using a close analogy between the complex representation of planar PH curves and the quaternion representation of spatial PH curves, this idea was later transformed to the spatial case in [34] where the Hermite C^1 interpolation scheme by spatial cubic PH biarcs was presented and a general algorithm for computing interpolants was designed, studied and applied.

In this paper, we will extend the ideas from [33, 34] to the C^2 Hermite interpolation by planar/spatial PH curves. Instead of using PH curves of degree 9 as in [29] we will consider PH triarcs, which enables us to drop the degree of the used PH curve to 5. In other words, the main idea is to join three arcs of PH quintics at two unknown points – the first curve interpolates given C^2 Hermite data at one side, the third one interpolates the same type of given data at the other side and the middle arc is joined together with C^2 continuity to the first and the third arc. The algorithm will be formulated firstly for planar PH quintic triarcs using complex representation. Then, a straightforward generalization to the quaternion representation yields an analogous algorithm for spatial PH quintic triarcs. The functionality of the designed technique will be demonstrated by several planar and spatial examples.

The paper is organized as follows. In the next section some preliminaries of the used theory are given. The C^2 Hermite planar interpolation problem is presented and an algorithm for computing such interpolants is given in the third section. In the fourth section the presented approach is generalized to the spatial case and the numerical examples which confirm the theoretical results are shown. The main results of the paper are summarized in the concluding section.

2. Preliminaries

In this section, we review fundamentals of the theory of planar and spatial Pythagorean-hodograph curves and their relation to complex numbers and quaternions, respectively.

2.1. Complex numbers and planar PH curves

Planar Pythagorean-hodograph curves were introduced in [2]. A polynomial parametric curve $\boldsymbol{p} = (x, y)^\top$ of degree n with the hodograph $\boldsymbol{h} = \boldsymbol{p}' = (x', y')^\top$ is a Pythagorean-hodograph curve (shortly PH curve) if the components of its hodograph $\boldsymbol{h}$ fulfill the condition

$$x'^2 + y'^2 = \sigma^2,$$

where σ is a polynomial. The main advantages of PH curves are that they possess rational offset curves and have (piecewise) polynomial arc-length function.

With the help of Kubota's theorem (see [2, 35]) hodographs of all planar polynomial PH curves can be expressed in the form

$$\begin{aligned} x' &= w(u^2 - v^2), \\ y' &= w(2u\,v) \end{aligned}$$

for some real non-zero polynomials u, v, w, where w is usually taken as a constant.

In many cases (and also in the follow-up sections), it is advantageous to use complex representation of points and curves in the plane to represent planar PH curves (see [36]). More precisely, points in the plane are identified with complex numbers in the complex plane and planar polynomial parametric curves are identified with complex-valued polynomials. Then, $\boldsymbol{p} = x + \mathbf{i}\, y$ is a PH curve iff there exists a complex polynomial $\boldsymbol{w} = u + \mathbf{i}\, v$, called the preimage, such that the hodograph $\boldsymbol{h}$ of $\boldsymbol{p}$ can be expressed in the form

$$\boldsymbol{h} = \boldsymbol{w}^2 = u^2 - v^2 + \mathbf{i}\, 2\, u\, v.$$

2.2. Quaternions and spatial PH curves

Similarly to the relation of planar PH curves and complex number/polynomials, spatial PH curves can be determined with the help of quaternion algebra. For a definition of quaternions and the description of standard operations in a quaternion space $\mathbb{H}$, the reader is kindly referred, e.g., to [15]. Here, only some less known facts about quaternions, which will be used in Section 4, are reviewed .

A standard multiplication on quaternions is not commutative, but it is possible to define a commutative multiplication. For a pair of quaternions $\mathcal{A}, \mathcal{B} \in \mathbb{H}$, we define

$$\mathcal{A} \star \mathcal{B} := \frac{1}{2}(\mathcal{A}\, \mathbf{i}\, \bar{\mathcal{B}} + \mathcal{B}\, \mathbf{i}\, \bar{\mathcal{A}}). \tag{1}$$

The result is always a pure quaternion which can be identified with a vector in $\mathbb{R}^3$. A notation $\mathcal{A}^{2\star} := \mathcal{A} \star \mathcal{A}$ will be used further on. The following lemmas review how linear and quadratic equations with respect to $\star$-operation can be solved (see [29] and [37], respectively).

Lemma 1. *Let $\mathcal{A}$ be a given pure quaternion and $\mathcal{B}$ a given non-zero quaternion. Then all solutions of a linear $\star$–equation $\mathcal{X} \star \mathcal{B} = \mathcal{A}$ form a one-parameter family*

$$\mathcal{X}(\alpha; \mathcal{B}, \mathcal{A}) := \frac{\overline{(\alpha + \mathcal{A})}\mathcal{B}\mathbf{i}}{\mathcal{B}\bar{\mathcal{B}}}, \quad \alpha \in \mathbb{R}.$$

Lemma 2. *Let $\mathcal{A}$ be a given pure quaternion. All solutions of a quadratic $\star$–equation $\mathcal{X}^{2\star} = \mathcal{A}$ form a one–parameter family*

$$\mathcal{X} := \mathcal{X}(\varphi; \mathcal{A}) := \mathcal{X}_p(\mathcal{A})\mathcal{Q}_\varphi, \quad \mathcal{Q}_\varphi := \cos\varphi + \mathbf{i}\, \sin\varphi, \ \ \varphi \in [-\pi, \pi), \tag{2}$$

where $\mathcal{X}_p(\mathcal{A})$ is a particular solution given by

$$\mathcal{X}_p(\mathcal{A}) := \begin{cases} \sqrt{\|\mathcal{A}\|}\, \dfrac{\frac{\mathcal{A}}{\|\mathcal{A}\|} + \mathbf{i}}{\left\| \frac{\mathcal{A}}{\|\mathcal{A}\|} + \mathbf{i} \right\|}, & \frac{\mathcal{A}}{\|\mathcal{A}\|} \neq -\mathbf{i}, \\ \sqrt{\|\mathcal{A}\|}\, \mathbf{k}, & \frac{\mathcal{A}}{\|\mathcal{A}\|} = -\mathbf{i}. \end{cases}$$

Further, it can be proved that for arbitrary quaternions $\mathcal{A}$ and $\mathcal{B}$ it holds

$$\mathcal{A}\mathcal{Q}_\varphi \star \mathcal{B}\mathcal{Q}_\psi = \mathcal{A}\mathcal{Q}_{\varphi-\psi} \star \mathcal{B} = \mathcal{A} \star \mathcal{B}\mathcal{Q}_{\psi-\varphi}. \tag{3}$$

Let us focus on spatial Pythagorean-hodograph curves now. Similarly to the planar case, a polynomial parametric curve $\boldsymbol{p} = (x, y, z)^\top$ of degree n with the hodograph $\boldsymbol{h} = \boldsymbol{p}' = (x', y', z')^\top$ is a spatial Pythagorean-hodograph curve if the components of $\boldsymbol{h}$ fulfill the condition

$$x'^2 + y'^2 + z'^2 = \sigma^2,$$

where σ is a polynomial. Analogously to the planar PH curves and their complex representation, it is advantageous to use quaternion algebra to represent spatial PH curves, where points in the space are identified with pure quaternions and spatial parametric polynomials are identified with pure quaternion polynomials. Then, $\boldsymbol{p} = x\, \mathbf{i} + y\, \mathbf{j} + z\, \mathbf{k}$ is a spatial PH curve iff there exists a quaternion polynomial $\mathcal{A} = u + v\, \mathbf{i} + p\, \mathbf{j} + q\, \mathbf{k}$, called the preimage, such that the hodograph $\boldsymbol{h}$ can be expressed in the form

$$\boldsymbol{h} = \mathcal{A}\, \mathbf{i}\, \bar{\mathcal{A}} = \mathcal{A}^{2\star}.$$

Note that quaternions $\mathcal{A}$ and $\mathcal{A}\, \mathcal{Q}_\varphi$ generate the same hodograph.

3. Planar interpolation problem and an algorithm

This section is devoted to the study of C^2 Hermite interpolation with planar quintic PH triarcs. An algorithm for finding such a quintic PH triarc for given Hermite data is provided and the approximation order of the method is analyzed.

3.1. Algorithm

In this section the interpolation problem by planar quintic PH triarcs is presented and an algorithm for computing the interpolants is given. Since the previous section shows that a planar PH curve is easily characterized by its complex preimage, vectors in $\mathbb{R}^2$ will be identified with complex numbers and vice versa.

Suppose that $\boldsymbol{A}, \boldsymbol{B} \in \mathbb{C}$ are two given points and $\boldsymbol{t}_A, \boldsymbol{t}_B \in \mathbb{C}$ are given associated tangent vectors. Additionally, let us prescribe two second derivative vectors $\boldsymbol{c}_A, \boldsymbol{c}_B \in \mathbb{C}$ at $\boldsymbol{A}, \boldsymbol{B}$ respectively. The goal is to find a C^2 continuous planar *quintic PH triarc* interpolant $\boldsymbol{p} : [\tau_0, \tau_3] \to \mathbb{C}$, composed of three planar quintic PH curves

$$\boldsymbol{p}_i : [\tau_{i-1}, \tau_i] \to \mathbb{C}, \quad i = 1, 2, 3,$$

with $\tau_0 < \tau_1 < \tau_2 < \tau_3$, i.e.,

$$\boldsymbol{p}(t) = \begin{cases} \boldsymbol{p}_1(t), & t \in [\tau_0, \tau_1], \\ \boldsymbol{p}_2(t), & t \in [\tau_1, \tau_2], \\ \boldsymbol{p}_3(t), & t \in [\tau_2, \tau_3], \end{cases} \tag{4}$$

satisfying

$$\boldsymbol{p}(\tau_0) = \boldsymbol{A}, \quad \boldsymbol{p}'(\tau_0) = \boldsymbol{t}_A, \quad \boldsymbol{p}''(\tau_0) = \boldsymbol{c}_A, \tag{5}$$

$$\boldsymbol{p}(\tau_3) = \boldsymbol{B}, \quad \boldsymbol{p}'(\tau_3) = \boldsymbol{t}_B, \quad \boldsymbol{p}''(\tau_3) = \boldsymbol{c}_B. \tag{6}$$

Since $\boldsymbol{p}$ should be in $C^2([\tau_0, \tau_3])$, we additionally require

$$\boldsymbol{p}_i^{(k)}(\tau_i) = \boldsymbol{p}_{i+1}^{(k)}(\tau_i), \quad i = 1, 2, \quad k = 0, 1, 2. \tag{7}$$

The interval values $\tau_0 < \tau_1 < \tau_2 < \tau_3$ are fixed but can be chosen arbitrarily. In all presented examples we have used the uniform division of the interval $[0, 1]$ at the points $1/3$ and $2/3$ but the interpolation algorithm works equally well for other values of τ_i's.

Parametric curves $\boldsymbol{p}_i$, $i = 1, 2, 3$, are assumed to be PH curves, so they are characterized by three associated preimage curves

$$\boldsymbol{w}_i(t) = \sum_{j=0}^{2} \boldsymbol{w}_{i,j}\, B_j^2\left(\frac{t - \tau_{i-1}}{\Delta\tau_{i-1}}\right) \quad i = 1, 2, 3,$$

where $\Delta\tau_{i-1} := \tau_i - \tau_{i-1}$, $i = 1, 2, 3$.

Let $\boldsymbol{p}_i$ be given in the Bernstein-Bézier basis as

$$\boldsymbol{p}_i(t) = \sum_{j=0}^{5} \boldsymbol{P}_{i,j}\, B_j^5\left(\frac{t - \tau_{i-1}}{\Delta\tau_{i-1}}\right), \quad i = 1, 2, 3.$$

By [15], the control points $\boldsymbol{P}_{i,j}$ are expressed by the control points of the preimages as

$$\begin{aligned} \boldsymbol{P}_{i,1} &= \boldsymbol{P}_{i,0} + \frac{\Delta\tau_{i-1}}{5}\boldsymbol{w}_{i,0}^2, \\ \boldsymbol{P}_{i,2} &= \boldsymbol{P}_{i,1} + \frac{\Delta\tau_{i-1}}{5}\boldsymbol{w}_{i,0}\,\boldsymbol{w}_{i,1}, \\ \boldsymbol{P}_{i,3} &= \boldsymbol{P}_{i,2} + \frac{\Delta\tau_{i-1}}{5}\left(\frac{2}{3}\boldsymbol{w}_{i,1}^2 + \frac{1}{3}\boldsymbol{w}_{i,0}\,\boldsymbol{w}_{i,2}\right), \\ \boldsymbol{P}_{i,4} &= \boldsymbol{P}_{i,3} + \frac{\Delta\tau_{i-1}}{5}\boldsymbol{w}_{i,1}\,\boldsymbol{w}_{i,2}, \\ \boldsymbol{P}_{i,5} &= \boldsymbol{P}_{i,4} + \frac{\Delta\tau_{i-1}}{5}\boldsymbol{w}_{i,2}^2. \end{aligned} \tag{8}$$

From (5), (6), (8) and some basic properties of Bézier curves we obtain

$$\boldsymbol{P}_{1,0} = \boldsymbol{A}, \quad \boldsymbol{w}_{1,0}^2 = \boldsymbol{t}_A, \quad \boldsymbol{w}_{1,0}\,\boldsymbol{w}_{1,1} - \boldsymbol{w}_{1,0}^2 = \frac{\Delta\tau_0}{4}\boldsymbol{c}_A, \tag{9}$$

and

$$\boldsymbol{P}_{3,5} = \boldsymbol{B}, \quad \boldsymbol{w}_{3,2}^2 = \boldsymbol{t}_B, \quad \boldsymbol{w}_{3,2}^2 - \boldsymbol{w}_{3,1}\,\boldsymbol{w}_{3,2} = \frac{\Delta\tau_2}{4}\boldsymbol{c}_B. \tag{10}$$

The continuity conditions at τ_1 and τ_2 clearly imply $\boldsymbol{P}_{2,0} = \boldsymbol{P}_{1,5}$ and $\boldsymbol{P}_{3,0} = \boldsymbol{P}_{2,5}$. This, together with (8), gives

$$\boldsymbol{P}_{2,0} = \boldsymbol{A} + \frac{\Delta\tau_0}{5}\left(\boldsymbol{w}_{1,0}^2 + \boldsymbol{w}_{1,0}\,\boldsymbol{w}_{1,1} + \frac{2}{3}\boldsymbol{w}_{1,1}^2 + \frac{1}{3}\boldsymbol{w}_{1,0}\,\boldsymbol{w}_{1,2} + \boldsymbol{w}_{1,1}\,\boldsymbol{w}_{1,2} + \boldsymbol{w}_{1,2}^2\right), \tag{11}$$

$$\boldsymbol{P}_{2,5} = \boldsymbol{B} - \frac{\Delta\tau_2}{5}\left(\boldsymbol{w}_{3,0}^2 + \boldsymbol{w}_{3,0}\,\boldsymbol{w}_{3,1} + \frac{2}{3}\boldsymbol{w}_{3,1}^2 + \frac{1}{3}\boldsymbol{w}_{3,0}\,\boldsymbol{w}_{3,2} + \boldsymbol{w}_{3,1}\,\boldsymbol{w}_{3,2} + \boldsymbol{w}_{3,2}^2\right). \tag{12}$$

Using (8) it follows that

$$\boldsymbol{P}_{2,5} - \boldsymbol{P}_{2,0} = \frac{\Delta\tau_1}{5}\left(\boldsymbol{w}_{2,0}^2 + \boldsymbol{w}_{2,0}\,\boldsymbol{w}_{2,1} + \frac{2}{3}\boldsymbol{w}_{2,1}^2 + \frac{1}{3}\boldsymbol{w}_{2,0}\,\boldsymbol{w}_{2,2} + \boldsymbol{w}_{2,1}\,\boldsymbol{w}_{2,2} + \boldsymbol{w}_{2,2}^2\right). \tag{13}$$

The first and the second order continuity conditions at τ_1 and τ_2 further imply

$$\boldsymbol{w}_{i,2}^2 = \boldsymbol{w}_{i+1,0}^2, \quad \frac{1}{\Delta\tau_{i-1}}\left(\boldsymbol{w}_{i,2}^2 - \boldsymbol{w}_{i,1}\,\boldsymbol{w}_{i,2}\right) = \frac{1}{\Delta\tau_i}\left(\boldsymbol{w}_{i+1,0}\,\boldsymbol{w}_{i+1,1} - \boldsymbol{w}_{i+1,0}^2\right), \quad i = 1, 2. \tag{14}$$

The equations (9)–(14) form a system of 11 complex equations for 11 complex unknowns $\boldsymbol{w}_{i,j}$, $i = 1, 2, 3$, $j = 0, 1, 2$, $\boldsymbol{P}_{2,0}$ and $\boldsymbol{P}_{2,5}$. From the equations (9), (10) and (14) we derive

$$\boldsymbol{w}_{1,0} = \chi_A\sqrt{\boldsymbol{t}_A}, \quad \boldsymbol{w}_{3,2} = \chi_B\sqrt{\boldsymbol{t}_B}, \quad \boldsymbol{w}_{1,2} = \chi_1\,\boldsymbol{w}_{2,0}, \quad \boldsymbol{w}_{3,0} = \chi_2\,\boldsymbol{w}_{2,2}, \tag{15}$$

where each of χ_A, χ_B, χ_1 and χ_2 is either 1 or -1, and consequently

$$\boldsymbol{w}_{1,1} = \frac{\boldsymbol{t}_A + \frac{\Delta\tau_0}{4}\boldsymbol{c}_A}{\chi_A\sqrt{\boldsymbol{t}_A}}, \quad \boldsymbol{w}_{3,1} = \frac{\boldsymbol{t}_B - \frac{\Delta\tau_2}{4}\boldsymbol{c}_B}{\chi_B\sqrt{\boldsymbol{t}_B}}. \tag{16}$$

From (14) it follows also

$$\boldsymbol{w}_{2,0} = \frac{\Delta\tau_0\,\Delta\tau_1}{\Delta\tau_0 + \Delta\tau_1}\left(\frac{1}{\Delta\tau_1}\boldsymbol{w}_{2,1} + \frac{1}{\Delta\tau_0}\frac{\chi_1}{\chi_A}\frac{\boldsymbol{t}_A + \frac{\Delta\tau_0}{4}\boldsymbol{c}_A}{\sqrt{\boldsymbol{t}_A}}\right), \tag{17}$$

$$\boldsymbol{w}_{2,2} = \frac{\Delta\tau_1\Delta\tau_2}{\Delta\tau_1 + \Delta\tau_2}\left(\frac{1}{\Delta\tau_1}\boldsymbol{w}_{2,1} + \frac{1}{\Delta\tau_2}\frac{\chi_2}{\chi_B}\frac{\boldsymbol{t}_B - \frac{\Delta\tau_2}{4}\boldsymbol{c}_B}{\sqrt{\boldsymbol{t}_B}}\right). \tag{18}$$

Here, we have assumed that $\boldsymbol{w}_{2,0} \neq \boldsymbol{0}$ and $\boldsymbol{w}_{2,2} \neq \boldsymbol{0}$, which should be fulfilled since we consider only regular quintic PH curves.
Considering (15)–(18) in (11)–(13), we end up with one complex quadratic equation for $\boldsymbol{w}_{2,1}$, namely

$$\sum_{i=1}^{3}\Delta\tau_{i-1}\left(\boldsymbol{w}_{i,0}^2 + \boldsymbol{w}_{i,0}\,\boldsymbol{w}_{i,1} + \frac{2}{3}\boldsymbol{w}_{i,1}^2 + \frac{1}{3}\boldsymbol{w}_{i,0}\,\boldsymbol{w}_{i,2} + \boldsymbol{w}_{i,1}\,\boldsymbol{w}_{i,2} + \boldsymbol{w}_{i,2}^2\right) - 5\,(\boldsymbol{B} - \boldsymbol{A}) = \boldsymbol{0}. \tag{19}$$

It is easy to see that the expressions (8) for the control points of the triarc segments involve only the products $\chi_1\,\chi_A$ or $\chi_2\,\chi_B$. Thus we can assume that, e.g., $\chi_1 = \chi_2 = 1$. We still have two possibilities for each of χ_A or χ_B, which together with two solutions of the quadratic equation for $\boldsymbol{w}_{2,1}$ gives eight solutions in general. But multiplying the control points of the preimage by -1 does not change the curve, thus we can, e.g., choose $\chi_A = 1$. This leaves four possible choices for the solution. Let them be denoted by $\boldsymbol{w}_{2,1}^{\pm,\pm}$, where the first symbol $\pm$ denotes the sign of the χ_B and the second one the sign in the solution of the the quadratic equation (19). Consequently, we obtain four possible interpolants, which will be denoted accordingly as $\boldsymbol{p}^{\pm,\pm}$.

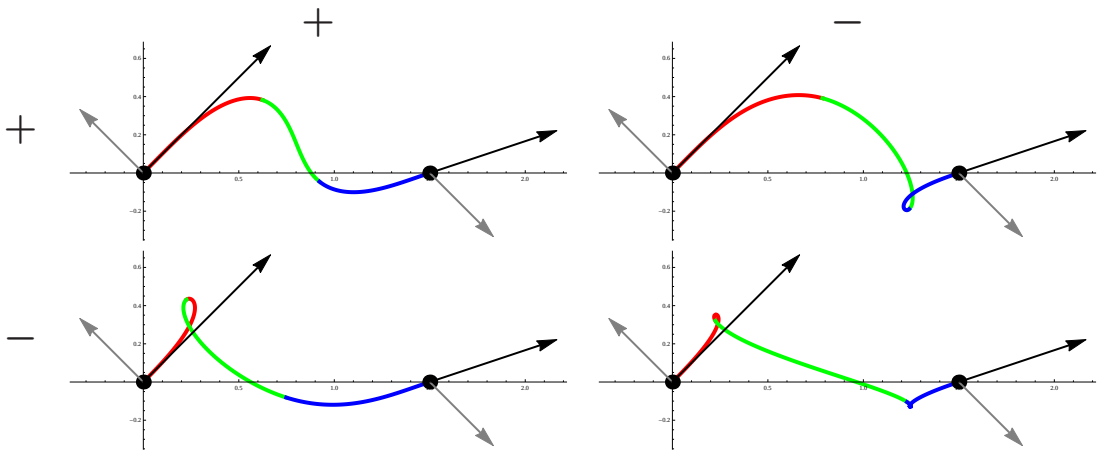

Figure 1: Four distinct quintic PH triarcs for input data in Example 1 labelled by $\boldsymbol{p}^{+,+}$ (top left), $\boldsymbol{p}^{+,-}$ (top right), $\boldsymbol{p}^{-,+}$ (bottom left) and $\boldsymbol{p}^{-,-}$ (bottom right).

Example 1. Let us consider C^2 Hermite data

$$\boldsymbol{P}_0 = (0,0)^\top,\ \boldsymbol{P}_2 = \left(\frac{3}{2},0\right)^\top,\quad \boldsymbol{t}_0 = (2,2)^\top,\ \boldsymbol{t}_2 = \left(2,\frac{2}{3}\right)^\top,\quad \boldsymbol{c}_0 = (-1,1)^\top,\ \boldsymbol{c}_2 = (1,-1)^\top.$$

With the help of the method described in the previous paragraphs we can find all four distinct quintic PH triarcs matching given data (see Fig. 1).

3.2. Asymptotic approximation order

In this section the approximation properties of all four interpolating triarcs will be analyzed. Let the data be sampled from an analytic parametric curve $\boldsymbol{f} : [0,h] \to \mathbb{C}$, $s \mapsto \boldsymbol{f}(s)$, parameterized by the arc-length and let $\varphi : [a,b] \to [0,h]$, $t \mapsto h\,(t-a)/(b-a)$, be a particular linear reparameterization. We can assume (without loss of generality) that $a = 0$ and $b = 1$ to simplify the analysis. Using the well-known Frenet-Serret formulae, the curve can be expressed as

$$\begin{aligned}\boldsymbol{f}(s) = s - \frac{1}{6}\kappa_0^2 s^3 - \frac{1}{8}\kappa_0\kappa_1 s^4 + \frac{1}{120}\left(\kappa_0^4 - 4\kappa_2\kappa_0 - 3\kappa_1^2\right)s^5 + \\ + \left(\frac{\kappa_0 s^2}{2} + \frac{\kappa_1 s^3}{6} + \frac{1}{24}\left(\kappa_2 - \kappa_0^3\right)s^4 + \frac{1}{120}\left(\kappa_3 - 6\kappa_0^2\kappa_1\right)s^5\right)\mathbf{i} + \mathcal{O}\left(h^6\right),\end{aligned} \tag{20}$$

where $\kappa(s) = \kappa_0 + \kappa_1 s + \frac{\kappa_2}{2!}s^2 + \frac{\kappa_3}{3!}s^3 + \mathcal{O}\left(s^4\right)$ is the Maclaurin series of the curvature of $\boldsymbol{f}$. The task is to construct the triarc (4) that satisfies (5) and (6) for the data

$$\begin{aligned}\boldsymbol{A} &= (\boldsymbol{f}\circ\varphi)(0) = 0,\quad \boldsymbol{t}_A = (\boldsymbol{f}\circ\varphi)'(0) = h,\quad \boldsymbol{c}_A = (\boldsymbol{f}\circ\varphi)''(0) = h^2\kappa_0\,\mathbf{i},\\ \boldsymbol{B} &= (\boldsymbol{f}\circ\varphi)(1) = h - \frac{1}{6}h^3\kappa_0^2 - \frac{1}{8}h^4\kappa_0\kappa_1 + \left(\frac{h^2\kappa_0}{2} + \frac{h^3\kappa_1}{6} + \frac{1}{24}h^4\left(\kappa_2 - \kappa_0^3\right)\right)\mathbf{i} + \mathcal{O}\left(h^5\right),\\ \boldsymbol{t}_B &= (\boldsymbol{f}\circ\varphi)'(1) = h - \frac{1}{2}h^3\kappa_0^2 - \frac{1}{2}h^4\kappa_0\kappa_1 + \left(h^2\kappa_0 + \frac{h^3\kappa_1}{2} + \frac{1}{6}h^4\left(\kappa_2 - \kappa_0^3\right)\right)\mathbf{i} + \mathcal{O}\left(h^5\right),\\ \boldsymbol{c}_B &= (\boldsymbol{f}\circ\varphi)''(1) = -h^3\kappa_0^2 - \frac{3}{2}h^4\kappa_0\kappa_1 + \left(h^2\kappa_0 + h^3\kappa_1 + \frac{1}{2}h^4\left(\kappa_2 - \kappa_0^3\right)\right)\mathbf{i} + \mathcal{O}\left(h^5\right)\end{aligned}$$

taken from the reparameterized curve $\boldsymbol{f}$. From (15)–(18) it follows that the control points of the preimage expressed with the unknown $\boldsymbol{w}_{2,1}$ expand as

$$\begin{aligned}
\boldsymbol{w}_{1,0} &= \sqrt{h}, \quad \boldsymbol{w}_{1,1} = \sqrt{h} + \frac{1}{4}h^{3/2}\kappa_0\tau_1\,\mathbf{i} + \mathcal{O}\left(h^{7/2}\right),\\
\boldsymbol{w}_{1,2} &= \frac{\tau_1\boldsymbol{w}_{2,1}}{\tau_2} + \sqrt{h}\left(1-\frac{\tau_1}{\tau_2}\right) - \frac{h^{3/2}\kappa_0\tau_1\left(\tau_1-\tau_2\right)}{4\tau_2}\mathbf{i} + \mathcal{O}\left(h^{7/2}\right),\\
\boldsymbol{w}_{2,0} &= \boldsymbol{w}_{1,2} + \mathcal{O}\left(h^{7/2}\right),\\
\boldsymbol{w}_{2,2} &= \frac{\left(\tau_2-1\right)\boldsymbol{w}_{2,1}}{\tau_1-1} + \frac{\sqrt{h}\left(\tau_1-\tau_2\right)\chi_B}{\tau_1-1} + \frac{h^{3/2}\kappa_0\left(\tau_1-\tau_2\right)\left(\tau_2+1\right)\chi_B}{4\left(\tau_1-1\right)}\mathbf{i} -\\
&\quad - \frac{h^{5/2}\left(\kappa_0^2-2\,\kappa_1\,\mathbf{i}\right)\left(\tau_1-\tau_2\right)\tau_2\chi_B}{8\left(\tau_1-1\right)} + \mathcal{O}\left(h^{7/2}\right),\\
\boldsymbol{w}_{3,0} &= \boldsymbol{w}_{2,2} + \mathcal{O}\left(h^{7/2}\right),\\
\boldsymbol{w}_{3,1} &= \sqrt{h}\chi_B + \frac{1}{4}h^{3/2}\kappa_0\left(\tau_2+1\right)\chi_B\,\mathbf{i} - \frac{1}{8}h^{5/2}\left(\kappa_0^2-2\,\kappa_1\,\mathbf{i}\right)\tau_2\chi_B + \mathcal{O}\left(h^{7/2}\right),\\
\boldsymbol{w}_{3,2} &= \sqrt{h}\chi_B + \frac{1}{2}h^{3/2}\kappa_0\chi_B\,\mathbf{i} - \frac{1}{8}h^{5/2}\left(\kappa_0^2-2\,\kappa_1\,\mathbf{i}\right)\chi_B + \mathcal{O}\left(h^{7/2}\right).
\end{aligned}$$

The equation (19) for $\boldsymbol{w}_{2,1}$ thus becomes $C_2(h)\boldsymbol{w}_{2,1}^2 + C_1(h)\boldsymbol{w}_{2,1} + C_0(h) = 0$, where

$$C_2(h) = \frac{\tau_1^2+\tau_2^2+\left(\tau_1-3\right)\tau_2}{15\left(\tau_1-1\right)\tau_2}, \quad C_1(h) = \mathcal{O}\left(\sqrt{h}\right), \quad C_0(h) = \mathcal{O}\left(h\right).$$

The solutions for $\chi_B = 1$ are

$$\begin{aligned}
\boldsymbol{w}_{2,1}^{+,+} &= \sqrt{h} + \frac{1}{4}\kappa_0\left(\tau_1+\tau_2\right)h^{3/2}\,\mathbf{i} - \frac{1}{8}\left(\kappa_0^2-2\,\kappa_1\,\mathbf{i}\right)\tau_1\tau_2h^{5/2} + \mathcal{O}\left(h^{7/2}\right),\\
\boldsymbol{w}_{2,1}^{+,-} &= \frac{\left(\tau_1^2-9\tau_2\tau_1+\tau_2\left(\tau_2+7\right)\right)}{\tau_1^2+\tau_2\tau_1+\left(\tau_2-3\right)\tau_2}\sqrt{h} + \kappa_0\frac{\tau_1^3-3\tau_2\tau_1^2-3\tau_2\left(\tau_2+1\right)\tau_1+\tau_2\left(\tau_2^2+2\tau_2+5\right)}{4\left(\tau_1^2+\tau_2\tau_1+\left(\tau_2-3\right)\tau_2\right)}h^{3/2}\,\mathbf{i} -\\
&\quad - \left(\kappa_0^2-2\,\kappa_1\,\mathbf{i}\right)\frac{\tau_2\left(\tau_2^2+\left(1-3\tau_1\right)\tau_2+1\right)}{8\left(\tau_1^2+\tau_2\tau_1+\left(\tau_2-3\right)\tau_2\right)}h^{5/2} + \mathcal{O}\left(h^{7/2}\right).
\end{aligned}$$

and for $\chi_B = -1$ are

$$\begin{aligned}
\boldsymbol{w}_{2,1}^{-,+} &= c_1^+(\tau_1,\tau_2)\sqrt{h} + \kappa_0c_2^+(\tau_1,\tau_2)h^{3/2}\,\mathbf{i} + \left(\kappa_0^2c_3^+(\tau_1,\tau_2) + \kappa_1c_4^+(\tau_1,\tau_2)\,\mathbf{i}\right)h^{5/2} + \mathcal{O}\left(h^{7/2}\right),\\
\boldsymbol{w}_{2,1}^{-,-} &= c_1^-(\tau_1,\tau_2)\sqrt{h} + \kappa_0c_2^-(\tau_1,\tau_2)h^{3/2}\,\mathbf{i} + \left(\kappa_0^2c_3^-(\tau_1,\tau_2) + \kappa_1c_4^-(\tau_1,\tau_2)\,\mathbf{i}\right)h^{5/2} + \mathcal{O}\left(h^{7/2}\right),
\end{aligned}$$

where $c_i^{\pm}(\tau_1,\tau_2)$, $i = 1,2,3,4$, denote some rather complicated expressions involving only τ_1 and τ_2. Suppose first that $\boldsymbol{w}_{2,1} = \boldsymbol{w}_{2,1}^{+,+}$. Then the triarc (4) expands as

$$\boldsymbol{p}_i^{+,+}(t) = ht + \frac{1}{2}\kappa_0t^2h^2\,\mathbf{i} - \frac{1}{6}\left(\kappa_0^2-\kappa_1\right)t^3h^3 + \pi_{4,i}(t;\tau_1,\tau_2,\kappa_0,\kappa_1,\kappa_2)h^4 + \mathcal{O}\left(h^5\right), \quad t\in[\tau_{i-1},\tau_i], \tag{21}$$

for $i = 1,2,3$, where $\pi_{4,i}$ is a complex polynomial in t of degree 4 with coefficients involving $\tau_1,\tau_2,\kappa_0,\kappa_1,\kappa_2$. From (21) and (20) then follows that

$$\|\boldsymbol{p}^{+,+} - \boldsymbol{f}\circ\varphi\| = \mathcal{O}\left(h^4\right),$$

i.e., the approximation order is equal to four. For the other three solutions the triarc (4) expands as

$$\boldsymbol{p}^{+,-}(t) = \pi_{5,i}^{+,-}(t;\tau_1,\tau_2)h + \mathcal{O}\left(h^2\right), \quad t\in[\tau_{i-1},\tau_i], \quad i = 1,2,3, \tag{22}$$

$$\boldsymbol{p}^{-,\pm}(t) = \pi_{5,i}^{-,\pm}(t;\tau_1,\tau_2)h + \mathcal{O}\left(h^2\right), \quad t\in[\tau_{i-1},\tau_i], \quad i = 1,2,3, \tag{23}$$

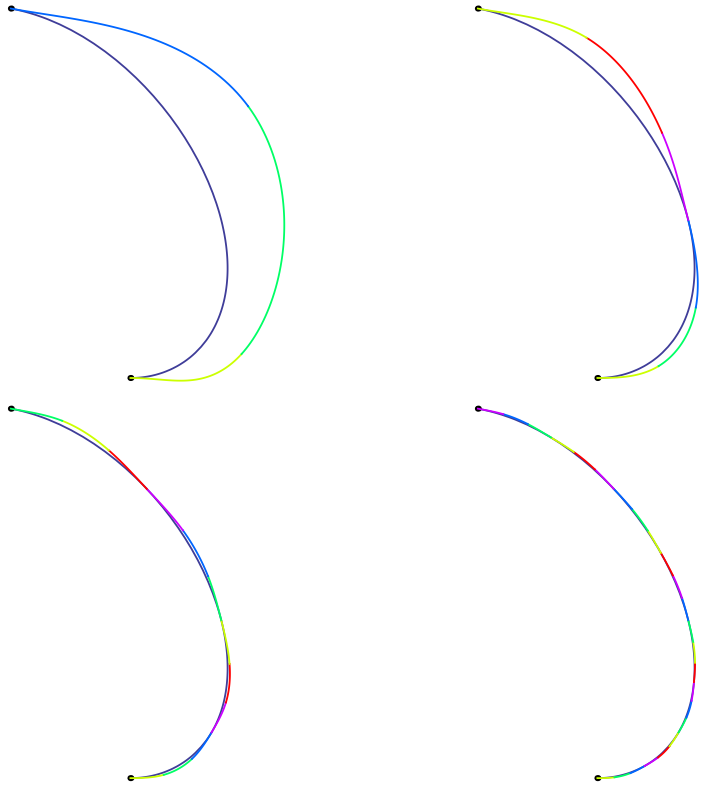

Figure 2: The curve defined in (24) and its approximation by C^2 PH quintic triarc for n segments: $n = 1$ (top left), $n = 2$ (top right), $n = 4$ (bottom left) and $n = 8$ (bottom right).

where $\pi_{5,i}^{+,-}$, $\pi_{5,i}^{-,+}$ and $\pi_{5,i}^{-,-}$ are complex polynomials in t of degree 5 with coefficients involving only τ_1 and τ_2. It can be checked that none of the polynomials can be equal to $t\,h$ for any $0 < \tau_1 < \tau_2 < 1$. Therefrom it follows that

$$\|\boldsymbol{p}^{+,-} - \boldsymbol{f} \circ \varphi\| = \mathcal{O}(h), \quad \|\boldsymbol{p}^{-,\pm} - \boldsymbol{f} \circ \varphi\| = \mathcal{O}(h),$$

which implies the approximation order one. Let us summarize the results in the following theorem.

Theorem 1. *Let $\boldsymbol{f} : [0, h] \to \mathbb{C}$, $s \mapsto \boldsymbol{f}(s)$ be an analytic complex curve and $\varphi : [0, 1] \to [0, h]$, $t \mapsto th$, a linear reparameterization. Moreover, by $\boldsymbol{p}^{\pm,\pm} : [0, 1] \to \mathbb{C}$ let us denote four interpolating triarcs defined by* (4)*, that satisfy*

$$\boldsymbol{p}^{\pm,\pm}(i) = (\boldsymbol{f} \circ \varphi)(i), \quad \left(\boldsymbol{p}^{\pm,\pm}\right)'(i) = (\boldsymbol{f} \circ \varphi)'(i), \quad \left(\boldsymbol{p}^{\pm,\pm}\right)''(i) = (\boldsymbol{f} \circ \varphi)''(i), \quad i = 0, 1.$$

Then for any τ_1, τ_2, $0 < \tau_1 < \tau_2 < 1$, the triarc $\boldsymbol{p}^{+,+}$ has the approximation order four, i.e.,

$$\left\|\boldsymbol{p}^{+,+} - \boldsymbol{f} \circ \varphi\right\| = \mathcal{O}\left(h^4\right).$$

For the other three triarcs, the approximation order is equal to one, i.e.,

$$\left\|\boldsymbol{p}^{+,-} - \boldsymbol{f} \circ \varphi\right\| = \mathcal{O}(h), \quad \left\|\boldsymbol{p}^{-,\pm} - \boldsymbol{f} \circ \varphi\right\| = \mathcal{O}(h).$$

To confirm the theoretical asymptotic results by an numerical example, let us choose a smooth complex curve $\boldsymbol{f}$ and a reparameterization φ as (see Fig. 2)

$$\begin{aligned} &\boldsymbol{f} : [0, h] \to \mathbb{C}, \quad s \mapsto \log(s + 1)\cos(2s) + \sqrt{s^2 + 1}\log(s + 1)\sin(2s)\,\mathbf{i}, \\ &\varphi : [0, 1] \to [0, h], \quad t \mapsto h\,t. \end{aligned} \tag{24}$$

The data becomes

$$\begin{aligned}\boldsymbol{A} &= (\boldsymbol{f}\circ\varphi)(0),\ \boldsymbol{t}_A = (\boldsymbol{f}\circ\varphi)'(0),\ \boldsymbol{c}_A = (\boldsymbol{f}\circ\varphi)''(0),\\ \boldsymbol{B} &= (\boldsymbol{f}\circ\varphi)(h),\ \boldsymbol{t}_B = (\boldsymbol{f}\circ\varphi)'(h),\ \boldsymbol{c}_B = (\boldsymbol{f}\circ\varphi)''(h),\end{aligned} \tag{25}$$

for some h small enough. Let $e^{\pm,\pm}(h) := \|\boldsymbol{p}^{\pm,\pm} - \boldsymbol{f}\circ\varphi\|_{\infty,[0,1]}$ denote the distance between the triarc $\boldsymbol{p}^{\pm,\pm}$ and the given curve. To determine the approximation order numerically, we assume that $e^{\pm,\pm}(h) \sim \text{const}\cdot h^{\gamma^{\pm,\pm}}$ and we estimate the decay exponent $\gamma^{\pm,\pm}$ by comparing the errors of interpolating triarcs for different values of h. In Table 1 the errors $e^{\pm,\pm}(h)$ are shown for all four triarcs and $h = 2^{-k}$, $k = 0, 1, \ldots, 7$. Moreover, the decay exponents computed from two consecutive measurements are shown too. Since $\gamma^{\pm,\pm}$ tends to the order of approximation as h approaches zero, the results confirm that the approximation order for $\boldsymbol{p}^{+,+}$ is four and for the other three solutions it is just one.

h	$e^{+,+}(h)$	$\gamma^{+,+}$	$e^{+,-}(h)$	$\gamma^{+,-}$	$e^{-,+}(h)$	$\gamma^{-,+}$	$e^{-,-}(h)$	$\gamma^{-,-}$
1	0.005653	/	0.3403	/	0.3506	/	0.2399	/
$\frac{1}{2}$	0.0002240	4.657	0.1140	1.578	0.1242	1.497	0.1075	1.158
$\frac{1}{4}$	0.00001375	4.026	0.04577	1.317	0.05314	1.225	0.05426	0.986
$\frac{1}{8}$	$1.174\cdot10^{-6}$	3.550	0.02292	0.998	0.02684	0.986	0.02775	0.967
$\frac{1}{16}$	$8.334\cdot10^{-8}$	3.816	0.01154	0.990	0.01379	0.961	0.01409	0.978
$\frac{1}{32}$	$5.422\cdot10^{-9}$	3.942	0.005798	0.993	0.007019	0.974	0.007103	0.988
$\frac{1}{64}$	$3.436\cdot10^{-10}$	3.980	0.002907	0.996	0.003545	0.985	0.003567	0.994
$\frac{1}{128}$	$2.160\cdot10^{-11}$	3.992	0.001456	0.998	0.001782	0.992	0.001788	0.997

Table 1: Distances $e^{\pm,\pm}(h)$ of the curve (24) from its triarc interpolants $\boldsymbol{p}^{\pm,\pm}$ and corresponding parameters $\gamma^{\pm,\pm}$ showing numerical values of the decay exponent. As it is clearly seen from the table, only the solution $\boldsymbol{p}^{+,+}$ gives fourth order approximation.

4. Spatial interpolation problem and algorithm

In this section, we will show that it is straightforward to generalize the previous algorithm to the spatial case. The approach presented is similar to the generalization of planar C^1 Hermite interpolation by uniform and non-uniform TC-biarcs (see [33]) to the spatial case (see [34]).

Recall from Section 2 that spatial PH curves can be generated with the help of quaternion polynomials. Therefore, points and vectors in $\mathbb{R}^3$ will be identified with pure quaternions and vice versa in the rest of this section. Let $\boldsymbol{A}$, $\boldsymbol{B}$, $\boldsymbol{t}_A$, $\boldsymbol{t}_B$, $\boldsymbol{c}_A$, $\boldsymbol{c}_B \in \mathbb{R}^3$ be pairs of given points, associated tangent vectors and second derivatives vectors, respectively. The task is to compute a C^2 continuous spatial quintic PH triarc

$$\boldsymbol{p} : [\tau_0,\tau_3] \to \mathbb{R}^3 : \boldsymbol{p}(t) = \begin{cases} \boldsymbol{p}_1(t), & t\in[\tau_0,\tau_1],\\ \boldsymbol{p}_2(t), & t\in[\tau_1,\tau_2],\\ \boldsymbol{p}_3(t), & t\in[\tau_2,\tau_3],\end{cases} \qquad \tau_0<\tau_1<\tau_2<\tau_3,$$

interpolating given Hermite data.

The modification of the planar to the spatial case is based on one principle: all complex numbers are replaced by quaternions and the standard multiplication of complex numbers is replaced by $\star$-operation defined on quaternions, see (1). The preimage $\mathcal{A}_i$ and the associated PH curves $\boldsymbol{p}_i$ are represented in the Bernstein-Bézier form as

$$\boldsymbol{p}_i(t) = \sum_{j=0}^{5} \boldsymbol{P}_{i,j}\, B_j^5\left(\frac{t-\tau_{i-1}}{\Delta\tau_{i-1}}\right), \quad \mathcal{A}_i(t) = \sum_{j=0}^{5} \boldsymbol{A}_{i,j}\, B_j^5\left(\frac{t-\tau_{i-1}}{\Delta\tau_{i-1}}\right), \quad i=1,2,3,$$

and it holds that

$$\begin{aligned}
\boldsymbol{P}_{i,1} &= \boldsymbol{P}_{i,0} + \frac{\Delta\tau_{i-1}}{5}\mathcal{A}_{i,0}^{2\star}, \qquad \boldsymbol{P}_{i,2} = \boldsymbol{P}_{i,1} + \frac{\Delta\tau_{i-1}}{5}\mathcal{A}_{i,0}\star\mathcal{A}_{i,1},\\
\boldsymbol{P}_{i,3} &= \boldsymbol{P}_{i,2} + \frac{\Delta\tau_{i-1}}{5}\left(\frac{2}{3}\mathcal{A}_{i,1}^{2\star} + \frac{1}{3}\mathcal{A}_{i,0}\star\mathcal{A}_{i,2}\right),\\
\boldsymbol{P}_{i,4} &= \boldsymbol{P}_{i,3} + \frac{\Delta\tau_{i-1}}{5}\mathcal{A}_{i,1}\star\mathcal{A}_{i,2}, \qquad \boldsymbol{P}_{i,5} = \boldsymbol{P}_{i,4} + \frac{\Delta\tau_{i-1}}{5}\mathcal{A}_{i,2}^{2\star}.
\end{aligned}$$

The interpolating conditions that determine the spatial triarc are of the same form as the conditions (9)–(14) for the planar case, only analogously modified. Clearly, $\boldsymbol{P}_{1,0} = \boldsymbol{A}$ and $\boldsymbol{P}_{3,5} = \boldsymbol{B}$. The first order continuity conditions in (9), (10) and (14) can be solved with the help of Lemma 2. Namely,

$$\mathcal{A}_{1,0} = \mathcal{X}(\varphi_A;\boldsymbol{t}_A), \quad \mathcal{A}_{3,2} = \mathcal{X}(\varphi_B;\boldsymbol{t}_B), \quad \mathcal{A}_{1,2} = \mathcal{A}_{2,0}\mathcal{Q}_{\varphi_1}, \quad \mathcal{A}_{3,0} = \mathcal{A}_{2,2}\mathcal{Q}_{\varphi_2}, \tag{26}$$

where φ_A, φ_B, φ_1 and φ_2 are free angular parameters. The equations for the interpolation of second derivatives at the boundary, analogous to (9) and (10), can be solved using Lemma 1. The unknowns

$$\mathcal{A}_{1,1} = \mathcal{X}\left(\alpha_1;\mathcal{A}_{1,0},\boldsymbol{t}_A + \frac{\Delta\tau_0}{4}\boldsymbol{c}_A\right), \quad \mathcal{A}_{3,1} = \mathcal{X}\left(\alpha_2;\mathcal{A}_{3,2},\boldsymbol{t}_B - \frac{\Delta\tau_2}{4}\boldsymbol{c}_B\right) \tag{27}$$

are determined with two new free parameters α_1 and α_2 involved. The second order continuity conditions at τ_1 and τ_2, presented in (14), simplify to

$$\begin{aligned}
\mathcal{A}_{2,0}\star\frac{1}{\Delta\tau_0}\left(\mathcal{A}_{2,0} - \mathcal{A}_{1,1}\mathcal{Q}_{-\varphi_1}\right) &= \mathcal{A}_{2,0}\star\frac{1}{\Delta\tau_1}\left(\mathcal{A}_{2,1} - \mathcal{A}_{2,0}\right),\\
\mathcal{A}_{2,2}\star\frac{1}{\Delta\tau_1}\left(\mathcal{A}_{2,2} - \mathcal{A}_{2,1}\right) &= \mathcal{A}_{2,2}\star\frac{1}{\Delta\tau_2}\left(\mathcal{A}_{3,1}\mathcal{Q}_{-\varphi_2} - \mathcal{A}_{2,2}\right),
\end{aligned}$$

which by following the planar case should determine the unknowns $\mathcal{A}_{2,0}$ and $\mathcal{A}_{2,2}$. This could be done by using Lemma 1 with two additional free parameters introduced. Instead we can take a particular solution which is to equate the quaternions on the right side of the star operation which gives

$$\mathcal{A}_{2,0} = \frac{1}{\Delta\tau_0+\Delta\tau_1}\left(\Delta\tau_0\mathcal{A}_{2,1} + \Delta\tau_1\mathcal{A}_{1,1}\mathcal{Q}_{-\varphi_1}\right), \quad \mathcal{A}_{2,2} = \frac{1}{\Delta\tau_1+\Delta\tau_2}\left(\Delta\tau_1\mathcal{A}_{3,1}\mathcal{Q}_{-\varphi_2} + \Delta\tau_2\mathcal{A}_{2,1}\right). \tag{28}$$

Finally, we end up with one quadratic $\star$-equation, analogous to (19), for the remaining control point $\mathcal{A}_{2,1}$ of the preimage:

$$\sum_{i=1}^{3}\Delta\tau_{i-1}\left(\mathcal{A}_{i,0}^{2\star} + \mathcal{A}_{i,0}\star\mathcal{A}_{i,1} + \frac{2}{3}\mathcal{A}_{i,1}^{2\star} + \frac{1}{3}\mathcal{A}_{i,0}\star\mathcal{A}_{i,2} + \mathcal{A}_{i,1}\star\mathcal{A}_{i,2} + \mathcal{A}_{i,2}^{2\star}\right) - 5\,(\boldsymbol{B}-\boldsymbol{A}) = \boldsymbol{0}. \tag{29}$$

Solving this equation with the help of Lemma 2 introduces another free angular parameter ψ. To sum up, the control points of the preimage quaternion curve are completely determined by (26)–(28) and by a solution of (29). They are expressed with seven free parameters $\varphi_A, \varphi_B, \varphi_1, \varphi_2, \alpha_1, \alpha_2, \psi$. However, analogously to [34], it is possible to prove with the help of (3) that one angular parameter is superfluous. We can choose e.g., $\psi = 0$. Note that the number of free parameters coincides with the difference between the number of equations and unknowns that are involved in $\mathcal{C}^2$ quintic triarc construction. Namely, each quintic PH curve is determined by 14 parameters, the quintic PH triarc thus has $p = 42$ parameters of freedom. Interpolation conditions give $e = 4\cdot 9 = 36$ equations, and the difference is $p - e = 6$. To sum up, for any non-degenerate spatial C^2 Hermite data there exists a six-parametric family of interpolating quintic PH triarcs $\boldsymbol{p}_\tau(t;\varphi_A,\varphi_B,\varphi_1,\varphi_2,\alpha_1,\alpha_2)$.

Example 2. Let us consider C^2 Hermite data

$$\boldsymbol{P}_0 = (2,1,1)^\top,\ \boldsymbol{P}_2 = (1,2,1)^\top, \quad \boldsymbol{t}_0 = (1,1,1)^\top,\ \boldsymbol{t}_2 = (1,1,-2)^\top \quad \boldsymbol{c}_0 = \left(\frac{1}{2},\frac{1}{2},0\right)^\top,\ \boldsymbol{c}_2 = \left(\frac{1}{2},-\frac{1}{2},0\right)^\top.$$

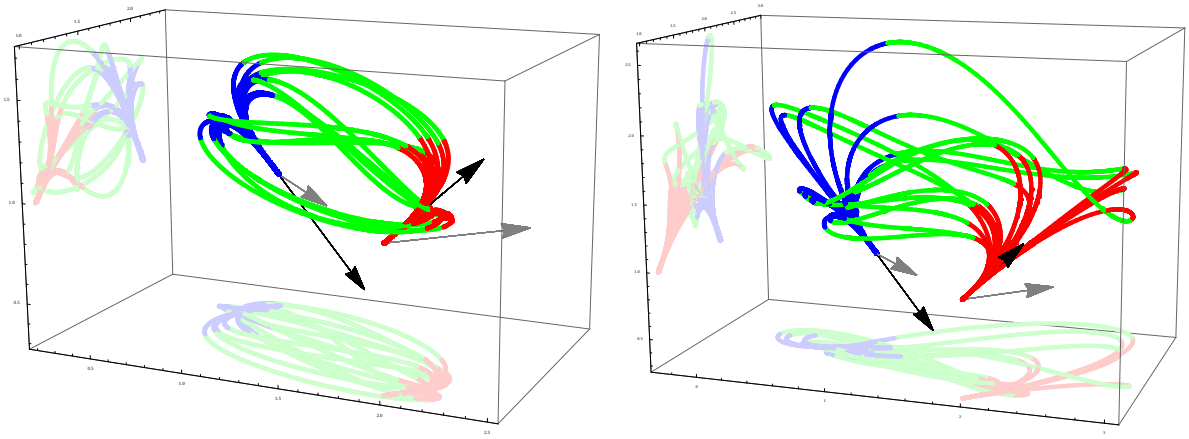

Figure 3: PH triarcs obtained for spatial input Hermite data in Example 2 (tangent vectors are scaled down by factor 3).

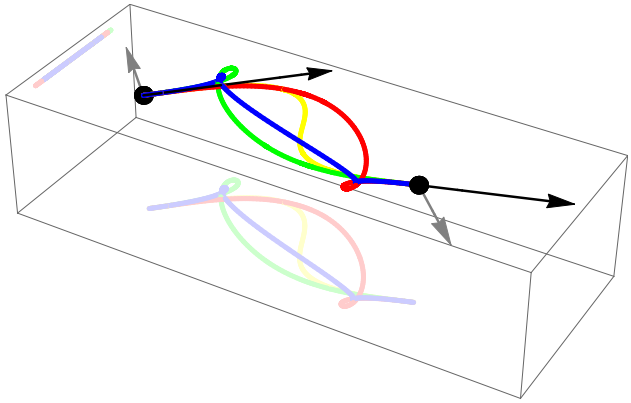

Figure 4: Uniform quintic PH triarcs obtained for planar input Hermite data in Example 3 (tangent vectors are scaled down by factor 3).

Fig. 3 (left) shows quintic PH triarcs obtained for pairs $\varphi_A, \varphi_B \in \{-\pi, -\frac{\pi}{2}, 0, \frac{\pi}{2}\}$ and $\varphi_1, \varphi_2, \alpha_1, \alpha_2$ equal to zero. Fig. 3 (right) shows quintic PH triarcs obtained for pairs $\alpha_1, \alpha_2 \in \{0, 2, 4, 6\}$, and parameters $\varphi_A, \varphi_B, \varphi_1, \varphi_2$ set to zero. In both cases, uniform quintic PH triarcs (i.e., $\tau_1 = \frac{1}{3}$, $\tau_2 = \frac{2}{3}$) are shown.

Analysis of this spatial algorithm is very similar to C^1 Hermite interpolation by spatial PH cubic biarcs (see [34]) and C^2 Hermite interpolation by PH curves of degree 9 (see [29]). With exactly the same reasoning as in [29, 34] it is possible to prove the following

Proposition 1. *For any planar C^2 Hermite data $\boldsymbol{P}_i$, $\boldsymbol{t}_i$, $\boldsymbol{c}_i$, $i = 0, 2$, the four quintic PH triarcs $\boldsymbol{p}_\tau(t; 0, 0, 0, 0, 0, 0)$, $\boldsymbol{p}_\tau(t; 0, -\pi, 0, 0, 0, 0)$, $\boldsymbol{p}_\tau(t; -\pi, 0, 0, 0, 0, 0)$, $\boldsymbol{p}_\tau(t; -\pi, -\pi, 0, 0, 0, 0)$ are planar and correspond to $\boldsymbol{p}^{\pm,\pm}$ solutions of the planar interpolation problem with quintic PH triarcs, presented in Section 3, respectively.*

PROOF. If we set $\alpha_1 = 0$, $\alpha_2 = 0$, $\varphi_1 = 0$ and $\varphi_2 = 0$, then the proof is completely analogous to the proofs of Proposition 1 in [34] and Theorem 3.11 in [29].

Example 3. Let us consider C^2 Hermite data

$$\boldsymbol{P}_0 = (0,0,0)^\top,\ \boldsymbol{P}_2 = \left(\frac{3}{2}, 0, 0\right)^\top, \quad \boldsymbol{t}_0 = (2,2,0)^\top,\ \boldsymbol{t}_2 = \left(2, \frac{2}{3}, 0\right)^\top \quad \boldsymbol{c}_0 = (-1,1,0)^\top,\ \boldsymbol{c}_2 = (1,-1,0)^\top.$$

Fig. 4 shows four quintic PH triarcs obtained for $\varphi_A, \varphi_B \in \{-\pi, 0\}$, parameters $\varphi_1, \varphi_2, \alpha_1, \alpha_2$ equal to zero and $\tau_1 = \frac{1}{3}$, $\tau_2 = \frac{2}{3}$. These solutions exactly correspond to the solutions of the planar problem.

Similarly as in the planar case one can analyze the asymptotic behaviour of the interpolating triarc in order to determine the set of parameters providing the best approximation order. By direct computation, analogously to the analysis of an approximation order in [34], the following theorem can be proved. Nevertheless, we will skip the details of the proof here, because expressions become much more complicated.

Theorem 2. *Let $\boldsymbol{f} : [0, h] \to \mathbb{H}$, $s \mapsto \boldsymbol{f}(s)$ be an analytic quaternion curve and $\varphi : [0, 1] \to [0, h]$, $t \mapsto th$, a linear reparameterization. Moreover, by $\boldsymbol{p}_\tau(t; \varphi_A, \varphi_B, \varphi_1, \varphi_2, \alpha_1, \alpha_2) : [0, 1] \to \mathbb{H}$ let us denote interpolating quintic PH triarcs that satisfy*

$$\begin{aligned} \boldsymbol{p}_\tau(t; \varphi_A, \varphi_B, \varphi_1, \varphi_2, \alpha_1, \alpha_2)\Big|_{t=i} &= (\boldsymbol{f} \circ \varphi)(i), \\ (\boldsymbol{p}_\tau(t; \varphi_A, \varphi_B, \varphi_1, \varphi_2, \alpha_1, \alpha_2))'\Big|_{t=i} &= (\boldsymbol{f} \circ \varphi)'(i), \\ (\boldsymbol{p}_\tau(t; \varphi_A, \varphi_B, \varphi_1, \varphi_2, \alpha_1, \alpha_2))''\Big|_{t=i} &= (\boldsymbol{f} \circ \varphi)''(i), \quad i = 0, 1. \end{aligned}$$

Then for any τ_1, τ_2, $0 < \tau_1 < \tau_2 < 1$, the triarc $\boldsymbol{p}_\tau(t; 0, 0, 0, 0, 0, 0)$ has the approximation order four, i.e.,

$$\|\boldsymbol{p}_\tau(t; 0, 0, 0, 0, 0, 0) - \boldsymbol{f} \circ \varphi\| = \mathcal{O}\left(h^4\right).$$

In the following example, we also give a numerical evidence of the above mentioned fact and we show that for other, non-zero, choices of the parameters φ_A, φ_B, the approximation order is generally only one.

Example 4. We are given an analytic curve $\boldsymbol{f}$ and a linear reparameterization φ,

$$\begin{aligned} &\boldsymbol{f} : [0, h] \to \mathbb{R}^3, \quad s \to \left(\log(s+1)\cos(s), \log(s+1)\sin(s), 1 + s^2\right)^\top, \\ &\varphi : [0, 1] \to [0, h], \quad t \to th. \end{aligned}$$

The data are sampled as (25) for some h small enough. Let $\tau_1 = \frac{1}{3}$, $\tau_2 = \frac{2}{3}$ and let $\boldsymbol{p}_\tau(t; 0, 0, 0, 0, 0, 0)$ denote the interpolating quintic PH triarc with all six parameters, $\varphi_A, \varphi_B, \varphi_1, \varphi_2, \alpha_1, \alpha_2$ set to zero. Furthermore, let $e(h) := \|\boldsymbol{p}_\tau - \boldsymbol{f} \circ \varphi\|_{\infty,[0,1]}$ denote the distance between the triarc $\boldsymbol{p}$ and the given curve. In Table 2 the errors e and the corresponding decay exponents γ are shown. The third column numerically indicates that for $\boldsymbol{p}_\tau(t; 0, 0, 0, 0, 0, 0)$ the approximation order of the curve approximation is four. In case when all free parameters are not set to zero, the approximation order falls. For example, let $\varphi_A = \frac{\pi}{2}, \varphi_B = -\frac{\pi}{2}, \varphi_1 = \varphi_2 = \alpha_1 = \alpha_2 = 0$. The associated errors and the decay exponents are presented in Table 2 which confirms that the approximation order for $\boldsymbol{p}_\tau(t; \frac{\pi}{2}, -\frac{\pi}{2}, 0, 0, 0, 0)$ is just one.

5. Conclusion

In this paper, the problem of C^2 Hermite interpolation of planar and spatial data (two points with associated first and second derivatives) by PH quintic triarcs was considered. More precisely, a PH quintic triarc curve was constructed by joining three PH quintics such that the first curve interpolates given C^2 Hermite data at one side, the third one interpolates the same type of given data at the other side and the middle arc is joined together with C^2 continuity to the first and the third arc. The method was formulated firstly for planar PH quintic triarcs using complex representation and consequently using the quaternion representation also for spatial PH quintic triarcs. For any set of C^2 planar boundary data we constructed four possible interpolants and, similarly, for any set of C^2 spatial boundary data we found a six-dimensional family of interpolating quintic PH triarcs. It was shown that that the best possible approximation order is 4. Several numerical examples were presented which confirmed that the constructed triarcs are of good shape and can be used for the approximation of planar/spatial parametric curves by PH quintic spline curves. One of the advantages of the proposed interpolation scheme is that it enables to drop the degree of the used PH curve from 9 to 5.

h	$\boldsymbol{p}_\tau\,(t;0,0,0,0,0,0)$		$\boldsymbol{p}_\tau\left(t;\frac{\pi}{2},-\frac{\pi}{2},0,0,0,0\right)$	
	$e(h)$	γ	$e(h)$	γ
1	0.002474	/	0.1519	/
$\frac{1}{2}$	0.0002292	3.432	0.03733	2.024
$\frac{1}{4}$	0.00001522	3.913	0.01301	1.521
$\frac{1}{8}$	$8.388\cdot 10^{-7}$	4.181	0.006332	1.038
$\frac{1}{16}$	$4.724\cdot 10^{-8}$	4.150	0.003142	1.011
$\frac{1}{32}$	$2.786\cdot 10^{-9}$	4.084	0.001567	1.004
$\frac{1}{64}$	$1.691\cdot 10^{-10}$	4.042	0.0007826	1.001
$\frac{1}{128}$	$1.042\cdot 10^{-11}$	4.021	0.0003912	1.001

Table 2: The approximation errors e and the corresponding decay exponents γ indicating the fourth order approximation for $\boldsymbol{p}_\tau\,(t;0,0,0,0,0,0)$ and just the first order approximation for $\boldsymbol{p}_\tau\left(t;\frac{\pi}{2},-\frac{\pi}{2},0,0,0,0\right)$.

Acknowledgments

All authors were supported by the Czech/Slovenian project KONTAKT MEB 091105. B. Bastl and K. Michálková were supported by Technology agency of the Czech Republic through the project TA03011157.

References

[1] I. R. Shafarevich, Basic algebraic geometry, Springer Verlag, 1974.
[2] R. Farouki, T. Sakkalis, Pythagorean hodographs, IBM J. Res. Dev. 34 (5) (1990) 736–752.
[3] R. Farouki, C. Neff, Hermite interpolation by Pythagorean-hodograph quintics, Math. Comp. 64 (212) (1995) 1589–1609.
[4] B. Jüttler, Hermite interpolation by Pythagorean hodograph curves of degree seven, Math. Comp. 70 (235) (2001) 1089–1111.
[5] F. Pelosi, M. Sampoli, R. Farouki, C. Manni, A control polygon scheme for design of planar C^2 PH quintic spline curves, Comput. Aided Geom. Design 24 (1) (2007) 28–52.
[6] R. Farouki, T. Sakkalis, Pythagorean-hodograph space curves, Adv. Comput. Math. 2 (1) (1994) 41–66.
[7] R. Farouki, T. Sakkalis, Rational space curves are not "unit speed", Comput. Aided Geom. Design 24 (4) (2007) 238–240.
[8] T. Sakkalis, R. T. Farouki, L. Vaserstein, Non-existence of rational arc length parameterizations for curves in R^n, J. Comput. Appl. Math. 228 (1) (2009) 494–497.
[9] T. Sakkalis, R. T. Farouki, Pythagorean-hodograph curves in Euclidean spaces of dimension greater than 3, J. Comput. Appl. Math. 236 (17) (2012) 4375–4382.
[10] H. Pottmann, Rational curves and surfaces with rational offsets, Comput. Aided Geom. Design 12 (2) (1995) 175–192.
[11] H. Pottmann, M. Peternell, Applications of Laguerre geometry in CAGD, Comput. Aided Geom. Design 15 (2) (1998) 165–186.
[12] M. Peternell, H. Pottmann, A Laguerre geometric approach to rational offsets, Comput. Aided Geom. Design 15 (3) (1998) 223–249.
[13] Z. Šír, B. Bastl, M. Lávička, Hermite interpolation by hypocycloids and epicycloids with rational offsets, Comput. Aided Geom. Design 27 (5) (2010) 405–417.
[14] R. T. Farouki, Z. Šír, Rational Pythagorean-hodograph space curves, Comput. Aided Geom. Design 28 (2) (2011) 75–88.
[15] R. T. Farouki, Pythagorean-hodograph curves: algebra and geometry inseparable, Vol. 1 of Geom. Comput., Springer, 2008.
[16] D. S. Meek, D. J. Walton, Geometric Hermite interpolation with Tschirnhausen cubics, J. Comput. Appl. Math. 81 (2) (1997) 299–309.
[17] G. Jaklič, J. Kozak, M. Krajnc, V. Vitrih, E. Žagar, On interpolation by planar cubic G^2 Pythagorean-hodograph spline curves, Math. Comp. 79 (269) (2010) 305–326.
[18] M. Byrtus, B. Bastl, G^1 Hermite interpolation by PH cubics revisited, Comput. Aided Geom. Design 27 (8) (2010) 622–630.
[19] E. Černohorská, Z. Šír, Support function of Pythagorean hodograph cubics and G^1 Hermite interpolation, in: B. Mourrain, S. Schaefer, G. Xu (Eds.), Advances in Geometric Modeling and Processing, Vol. 6130 of Lecture Notes in Comput. Sci., Springer Berlin / Heidelberg, 2010, pp. 29–42.
[20] H. P. Moon, R. T. Farouki, H. I. Choi, Construction and shape analysis of PH quintic Hermite interpolants, Comput. Aided Geom. Design 18 (2) (2001) 93–115.
[21] Z. Šír, R. Feichtinger, B. Jüttler, Approximating curves and their offsets using biarcs and Pythagorean hodograph quintics, Comput. Aided Design 38 (6) (2006) 608–618.
[22] G. Albrecht, R. T. Farouki, Construction of C^2 Pythagorean-hodograph interpolating splines by the homotopy method, Adv. Comput. Math. 5 (4) (1996) 417–442.
[23] H. I. Choi, R. T. Farouki, S.-H. Kwon, H. P. Moon, Topological criterion for selection of quintic Pythagorean-hodograph Hermite interpolants, Comput. Aided Geom. Design 25 (6) (2008) 411–433.

[24] B. Jüttler, C. Mäurer, Cubic Pythagorean-hodograph spline curves and applications to sweep surface modeling, Comput. Aided Design 31 (1) (1999) 73–83.
[25] F. Pelosi, R. T. Farouki, C. Manni, A. Sestini, Geometric Hermite interpolation by spatial Pythagorean-hodograph cubics, Adv. Comput. Math. 22 (4) (2005) 325–352.
[26] S.-H. Kwon, Solvability of G^1 Hermite interpolation by spatial Pythagorean-hodograph cubics and its selection scheme, Comput. Aided Geom. Design 27 (2) (2010) 138–149.
[27] G. Jaklič, J. Kozak, M. Krajnc, V. Vitrih, E. Žagar, An approach to geometric interpolation by Pythagorean-hodograph curves, Adv. Comput. Math. 37 (1) (2012) 123–150.
[28] Z. Šír, B. Jüttler, Spatial Pythagorean hodograph quintics and the approximation of pipe surfaces, in: R. Martin, H. Bez, M. Sabin (Eds.), Mathematics of Surfaces XI, Vol. 3604 of Lecture Notes in Comput. Sci., Springer Berlin Heidelberg, 2005, pp. 364–380.
[29] Z. Šír, B. Jüttler, C^2 Hermite interpolation by Pythagorean hodograph space curves, Math. Comp. 76 (259) (2007) 1373–1391.
[30] R. T. Farouki, C. Giannelli, C. Manni, A. Sestini, Identification of spatial PH quintic Hermite interpolants with near-optimal shape measures, Comput. Aided Geom. Design 25 (4-5) (2008) 274–297.
[31] R. T. Farouki, C. Manni, A. Sestini, Spatial C^2 PH quintic splines, in: T. Lyche, M. Mazure, L. Schumaker (Eds.), Curve and Surface Design: St. Malo 2002, Nashboro Press, Brentwood, 2003, pp. 147–156.
[32] R. T. Farouki, J. Peters, Smooth curve design with double-Tschirnhausen cubics, Ann. Numer. Math. 3 (1-4) (1996) 63–82.
[33] B. Bastl, K. Slabá, M. Byrtus, Planar C^1 Hermite interpolation with uniform and non-uniform TC-biarcs, Comput. Aided Geom. Design 30 (1) (2013) 58–77.
[34] B. Bastl, M. Bizzarri, M. Krajnc, M. Lávička, K. Slabá, Z. Šír, V. Vitrih, E. Žagar, C^1 Hermite interpolation with spatial Pythagorean-hodograph cubic biarcs, J. Comput. Appl. Math. 257 (0) (2014) 65–78.
[35] K. Kubota, Pythagorean triples in unique factorization domains, Amer. Math. Monthly 79 (5) (1972) 503–505.
[36] R. T. Farouki, The conformal map $z \to z^2$ of the hodograph plane, Comput. Aided Geom. Design 11 (4) (1994) 363–390.
[37] R. T. Farouki, M. al Kandari, T. Sakkalis, Hermite interpolation by rotation-invariant spatial Pythagorean-hodograph curves, Adv. Comput. Math. 17 (4) (2002) 369–383.